USAFETAC/PR--91/018

OPTIMAL PLACEMENT OF A GEODSS (GROUND-BASED ELECTROOPTICAL DEEP-SPACE SURVEILLANCE) SENSOR

by

CAPT ANTHONY J. WARREN

AUGUST 1991

USAF
ENVIRONMENTAL TECHNICAL
APPLICATIONS CENTER

Scott Air Force Base, Illinois, 62225-5438

REVIEW AND APPROVAL STATEMENT

USAFETAC/PR-91/018, *Optimal Placement of a GEODSS (Ground-Based Electrooptical Deep-Space Surveillance) Sensor*, August 1991, has been reviewed and is approved for public release. There is no objection to unlimited distribution of this document to the public at large, or by the Defense Technical Information Center (DTIC) to the National Technical Information Service (NTIS).

PATRICK J. BREITLING
Chief Scientist

FOR THE COMMANDER

WALTER S. BURGMANN
Scientific and Technical Information
Program Manager
30 August 1991

REPORT DOCUMENTATION PAGE

2. Report Date: August 1991

3. Report Type: Project Report

4. Title: Optimal Placement of a GEODSS (Ground-Based Deep Space Surveillance) Sensor

6. Author: Capt Anthony J. Warren

7. Performing Organization Name and Address: USAF Environmental Technical Applications Center (USAFETAC/DNY), Scott AFB, IL 62225-5438

8. Performing Organization Report Number: USAFETAC/PR--91/018

12. Distribution/Availability Statement: Approved for public release; distribution is unlimited.

13. Abstract: Successful operation of the Ground-Based Electrooptical Deep-Space Surveillance (GEODSS) system, basically an optical video camera that tracks objects in high Earth orbit, requires that the following five conditions are met: Sun at least 6 degrees below horizon; surface wind speed less than 25 knots; temperature more than -50° C; satellite elevation at least 15° above horizon; and a 5-minute cloud-free line-of-sight between satellite and sensor. This report gives the probabilities of combinations of those conditions at twelve proposed Canadian GEODSS sites. It includes a review of fundamentals, a discussion of computer model results, and a comparison of results for each candidate location

14. Subject Terms: SPACE, SPACE SURVEILLANCE, DEEP SPACE, SPACE OBJECTS, OPTICAL INSTRUMENTS, OPTICAL DETECTORS, OPTICAL TRACKING, ELECTROOPTICS, ENVIRONMENTS, AEROSPACE ENVIRONMENTS, VIDEO CAMERA

15. Number of Pages: 26

17. Security Classification of Report: Unclassified

18. Security Classification of this Page: Unclassified

19. Security Classification of Abstract: Unclassified

20. Limitation of Abstract: UL

Standard Form 298

PREFACE

This report documents work on USAFETAC Project #900833 in response to a support assistance request (SAR) from a Canadian AFIT student (Maj Pete Forgues) through Detachment 1, 2d Weather Squadron (ASD/WE), Wright-Patterson AFB, OH 45433-6503.

The SAR asked for the relative probabilities of certain environmental conditions at 12 Canadian locations, each a candidate for a Ground-Based Electrooptical Deep-Space Surveillance (GEODSS) sensor. The potential GEODSS sites span the Canadian landmass and represent all climates. Four GEODSS systems are installed now, with another (GEODSS-5) scheduled for Portugal.

Canada's participation in the space surveillance mission dates to 1961 with installation of the first Canadian Baker-Nunn system (an optical film camera) at Cold Lake, Alberta. In 1976, a second Baker-Nunn station was installed at St Margarets, New Brunswick. At the request of SPACECOM CINC, the Canadian Forces have agreed to operate the Baker-Nunn System at St Margarets until GEODSS-5 is operational.

Canadian participation in the space surveillance mission (by locating GEODSS sensors in Canada) once GEODSS-5 is operational is being debated by USSPACECOM and Canadian National Defence Headquarters (NDHQ). The NDHQ Directorate of Air Requirements, therefore, has asked that the best GEODSS (and GEODSS-like) locations in Canada be determined. This study concludes which sites are best and worst, and why.

Project analyst was Capt Anthony J. Warren, USAFETAC/DNY, DSN 576-5412.

CONTENTS

FIGURES

TABLES

1. INTRODUCTION

1.1 The GEODSS Sensor. The military mission of space surveillance is to detect, track, identify, and catalog man-made objects in space (USSPACECOMR 55-12). Radar is used to track objects in low-earth orbits (typically up to 5,000 km, but actual altitude varies depends on the type of radar). For objects at high altitudes, a global network of ground-based sensors provides observational data to the Space Surveillance Center (SSC) located at the Cheyenne Mountain complex, Colorado Springs, CO. The SSC analyzes surveillance data to determine the locations of orbiting satellites.

The sensor used for high-altitude orbit detection is the Ground-Based Electrooptical Deep-Space Surveillance (GEODSS) system, basically an optical video camera. Four GEODSS systems around the globe are currently operational, and a fifth system is scheduled for Portugal. The installation of a sixth system in Canada is being considered by the United States Space Command (USSPACECOM) and the Canadian National Defence Headquarters (NDHQ), whose Directorate for Air Requirements is seeking to determine the best Canadian GEODSS locations.

1.2 Environmental Effects on GEODSS. Determining the best locations requires evaluating many criteria; these include logistics, personnel support, and environmental effects. The last (the environment) is critical because weather elements have a significant effect on GEODSS operation. For example, low temperatures and high winds prevent the exposure and operation of the antenna system. For successful detection, a cloud-free line-of-sight must be present. And since the system tracks satellites based on infrared emissions, it can only work at night. Therefore, all the following conditions (*A*-*E*) must be met for successful detection of an orbiting satellite:

A ... The Sun is at least 6 degrees below the horizon.

B... The surface wind speed is less than 25 knots.

C... The temperature is more than -50° C.

D... The satellite elevation is at least 15° above the horizon.

E... There is a 5-minute cloud-free line-of-sight (CFLOS) between sensor and satellite.

1.3 Summary. This report presents probabilities of various combinations of the conditions described by *A* through *E*. The most important of these is the probability of condition *E*, given the joint occurrence of conditions *A*, *B*, *C*, and *D*. This value describes the probability of successful detection of the satellite given that it is in view, that temperature and wind conditions are favorable, and that it is dark enough. The methodology used to estimate these probabilities is also presented. Six satellite orbits are considered: an orbiting satellite at 19,000 km with a right ascension angle of 65° (a constellation of navigational satellites populates this orbit); and five geostationary orbits with the satellite located at 50° W, 70° W, 100° W, 120° W, and 140° W. Figure 1 lists the 12 stations for which probabilities are determined and gives their locations.

STATION	Latitude (Deg Min)	Longitude (Deg Min)	Block Station Number
Sandspit, British Columbia	53° 15' N	131° 49' W	711010
Churchill, Manitoba	58° 45' N	94° 05' W	719130
Penticton, British Columbia	49° 28' N	119° 36' W	718890
Chatham, New Brunswick	47° 01' N	65° 27' W	717170
Torbay, Newfoundland	47° 38' N	52° 42' W	718010
Alert, Northwest Territories	82° 30' N	62° 20' W	710820
Frobisher, Northwest Territories	63° 45' N	68° 34' W	719090
Inuvik, Northwest Territories	68° 18' N	133° 29' W	719570
London, Ontario	43° 02' N	81° 09' W	716230
Moose Jaw, Saskatchewan	50° 20' N	105° 33' W	718640
Whitehorse, Yukon Territories	60° 42' N	135° 07' W	719650
Cold Lake, Alberta	54° 25' N	110° 17' W	711120

Figure 1. Twelve proposed sites for placement of a GEODSS sensor.

2. FUNDAMENTALS

2.1 Cloud-Free Line-of-Sight. One of the requirements for successful GEODSS detection of an orbiting satellite is that there be a 5-minute cloud-free line-of-sight (CFLOS) between sensor and satellite. The climatological probability of CFLOS, therefore, is fundamental to evaluating the operational potential of a proposed GEODSS station. Because CFLOS is not reported in weather observations, a simulation model is required to estimate probabilities.

2.2 Statistical Models.

2.2.1 Cloud Cover Distribution. Malick et al. (1979) developed a model (hereafter referred to as the "Stanford Research Institute" or "SRI" model) for estimating CFLOS probability given two variables: fraction of sky covered by cloud, and viewing angle. However, sky cover is not routinely reported in some weather observation codes; in Canada, for example, where airways is the principal observing code, sky conditions are reported as clear, scattered, broken, or overcast. These airways reports are used to estimate the elements of a frequency distribution of sky cover known as the "Burger Aerial Algorithm" (Burger, 1985). The parameters of the Burger distribution are mean sky cover and sky dome scale distance. Table 1 lists the observed frequency of airways sky-cover categories for Moose Jaw at two different times: January 12Z and July 12Z. Table 1 also shows Burger distribution frequencies for 12 sky-cover categories. A plot of the Burger distribution is shown in Figure 2.

Table 1. Comparison of Moose Jaw cloud cover frequency distribution, 12Z January and 12Z July between airways categories and Burger distribution categories. Also listed are the Burger distribution parameters.

AIRWAYS OBSERVATIONS FOR MOOSE JAW

	CLR	SCT	BKN	OVC	Mean Sky Cover	Scale Distance
12Z January	0.296	0.191	0.162	0 350	0.529	2.444
12Z July	0.042	0.473	0.381	0.104	0.488	0.781

BURGER DISTRIBUTION FOR MOOSE JAW

Sky Cover Interval	12Z January	12Z July
0 00 - 0.05	0 261	0 067
0.06 - 0.15	0.074	0.127
0.16 - 0.25	0.039	0.085
0.26 - 0.35	0.037	0.082
0.36 - 0.45	0 028	0.076
0.46 - 0.55	0.031	0.078
0.56 - 0 65	0.031	0.078
0.66 - 0.75	0 028	0.074
0.76 - 0.85	0.038	0.079
0.86 - 0.95	0.041	0.080
0.96 - 1 00	0.392	0.174

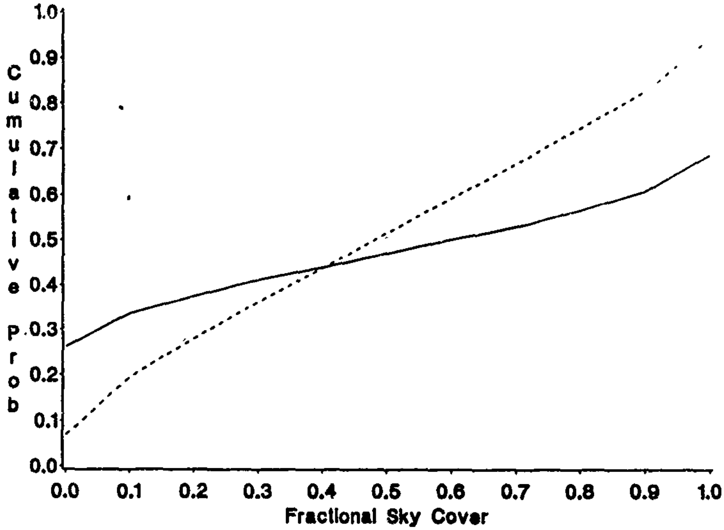

Figure 2. Cumulative distribution of cloud cover at Moose Jaw, 12Z January and 12Z July.

2.2.2 Transnormalization. The Burger distribution, which describes the frequency of sky cover categories, is the fundamental component of the USAFETAC Cloud Scene Generator (CLDGEN) simulation model developed to simulate a cloud scene at a particular time and location (Rupp, 1990). A detailed technical report on this model is in preparation, but a brief description is provided here.

Sky cover at any given time can be simulated using the Burger distribution and a random number generator. However, in order to compute a time series of observations, some technique must be employed to ensure that the simulated data show the proper serial correlation. The mathematical treatment of correlation between probability distributions is relatively straightforward when the distributions are normal. A normal approximation to the Burger distribution would be invalid in all but a few select cases. The advantages offered by normal distributions can be retained through a process known as "transnormalization" (Boehm, 1976). In Figure 2, the cumulative probability of obtaining a sky cover of 0.25 or less at Moose Jaw, Canada, (12Z January) or less is 37.4 percent. For a normal random variable with mean of zero and variance of unity, the value corresponding to the same cumulative probability is -0.734. This value is known as the "equivalent normal deviate" (END). Therefore, the initial sky cover at a particular point can be obtained by generating a random normal deviate; for example, 0.376. The corresponding cumulative probability for the value is 64.7 percent. Referring to Figure 2, this cumulative probability corresponds to a sky cover of nine-tenths. This is the first simulated sky cover observation; the simulated observation for the next time increment can be generated by the Ornstein-Uhlenbeck equation (Whiton and Berecek, 1982):

$$y_{t+\Delta t} = \rho_{\Delta t} y_t + \eta \sqrt{1 - \rho_{\Delta t}^2} \qquad (1)$$

where: $\hat{y}_t$ is the initial END

$\hat{y}_{t+\Delta t}$ is the END at the next time step

$\rho_{\Delta t}$ is the serial correlation for the time period Δt

η is a random normal deviate.

2.2.3 Serial Correlation. Assumptions about the nature of the serial correlation are necessary to obtain a value for $\rho_{\Delta t}$. It is generally assumed that meteorological phenomena are first-order Markov processes. For such processes the correlation is given by (Hering, 1989):

$$\rho_{\Delta t} = e^{-\Delta t/\tau} \tag{2}$$

where τ is referred to as the "relaxation time." A typical value of τ is 16 hours, which yields an hour-to-hour correlation of 0.94. It should be pointed out that τ refers to the temporal correlation between the ENDs of cloud cover--not the actual values of cloud cover.

2.3 Boehm Sawtooth Wave Model. The CLDGEN model generates a sky scene given an observation of mean sky cover. For specified azimuth and zenith angles, the model will generate either a value of CLOUD or NO CLOUD. It accomplishes this calculation in several steps. Based on the mean sky cover and zenith angle, the probability of CFLOS is obtained from the SRI model. The END of this probability is considered the threshold END. For each point of interest in the sky scene, a random normal deviate is generated; if it exceeds the threshold END, the sky cover value at this point is CLOUD--if not, the value is NO CLOUD.

In generating a cloud scene, the values of CLOUD and NO CLOUD must correspond to the observed spatial correlation, which is obtained by generating a field of correlated random deviates through a procedure referred to as the "Boehm sawtooth wave model" (Gringorten and Boehm, 1987). A recent version of this model, the four-dimensional sawtooth, is capable of generating not only three-dimensional spatial correlation, but also the temporal correlation described above with the Ornstein-Uhlenbeck equation. Two types of serial correlation can be defined. The first is the hour-to-hour correlation of reported sky cover. The second is the time correlation of cloud or no cloud conditions at a given point in the sky. A typical value for the first correlation is 16 hours, while the second is much shorter--about 30 minutes (Hering, 1989). While the correlation structure generated by a single sawtooth wave is not a Markov-type function, a correlation structure that approximates a Markov decay can be generated by adding together sawtooth waves of various wavelengths. Discussion of spatial correlation is more complex. The spatial correlation structure of the sawtooth wave model is given by Gringorten and Boehm (1987):

$$\rho_s = 1 - 8s/\pi + (3/2)s^2 \tag{3}$$

where ρ_s is the spatial correlation and s is the standardized separation distance. The last value is given by the actual distance divided by the sawtooth wavelength, λ. The sawtooth wavelength is an empirical parameter. Boehm (personal communication)[1] recommends the relation:

$$\lambda = 213r \tag{4}$$

where r is the sky-dome correlation scale distance, defined as the distance over which the correlation decreases to 0.99. The recommended value of this parameter for observations of sky cover is 7.2 km. For individual cloud elements, the CLDGEN model assumes that all clouds occur in a single layer at an arbitrary height of 15,000 feet

[1] Albert R. Boehm, ST Systems Corp., 109 Massachusetts Ave, Lexington, MA 01730

MSL. At this level, the length scale of cloud elements is on the order of 10^{-3}, that of synoptic-scale events; we therefore assumed a value of 0.0072 km for the sky-dome correlation scale distance.

2.4 Estimating CFLOS Probabilities. The CLDGEN model was used to predict the 5-minute probability of CFLOS between a point at the surface and an orbiting satellite. A separate subroutine provided the azimuth and elevation angle of the satellite as viewed from the ground. CLDGEN is then used to determine whether the point in the sky corresponding to the satellite location is cloud-free or not. The clock is then advanced 10 seconds and the process repeated. The number of completely clear 5-minute intervals divided by the total number of 5-minute intervals represents the climatological probability of obtaining a 5-minute CFLOS. The simulation is then run for several years (usually 10) to obtain stable statistics.

2.5 Sun-angle Constraint. Since the GEODSS is a passive electrooptical system, it can operate only in darkness; specifically, when the sun is below an elevation angle of 6 degrees (defined in Section 1 as condition *A*) This condition corresponds to the period between the end of evening civil twilight (EECT) and the beginning of morning civil twilight (BMCT). Table 2 depicts the monthly median fraction of time this event occurs. Subsequent probabilities are then computed given that condition *A* is occurring. At the high-latitude stations shown below, there are long periods when civil twilight does not end; between the inclusive dates shown, $P(A)=0$. In addition, civil twilight does not occur at Alert between 29 October and 12 February, during this period, $P(A)=1$.

- Alert 25 March - 19 September
- Frobisher 21 May - 23 July
- Inuvik 4 May - 10 August
- Whitehorse 15 June - 27 June

TABLE 2. Median fraction of time that the Sun is at least 6 degrees below the horizon, by month.

	JAN	FEB	MAR	APR	MAY	JUN	JUL	AUG	SEP	OCT	NOV	DEC
Sandspit	0.61	0.54	0.46	0.37	0.28	0.22	0.24	0.33	0.42	0.51	0.52	0.63
Churchill	0.64	0.55	0.46	0.34	0.22	0.12	0.16	0.28	0.40	0.51	0.61	0.66
Penticton	0.59	0.53	0.46	0.38	0.31	0.26	0.28	0.35	0.43	0.50	0.57	0.61
Chatham	0.58	0.53	0.46	0.39	0.32	0.28	0.29	0.36	0.43	0.50	0.57	0.60
Torbay	0.58	0.53	0.46	0.39	0.32	0.28	0.29	0.36	0.43	0.50	0.57	0.60
Alert	1.00	0.85	0.33	0.00	0.00	0.00	0.00	0.00	0.17	0.61	1.00	1.00
Frobisher	0.68	0.57	0.45	0.30	0.11	0.00	0.00	0.23	0.37	0.52	0.64	0.71
Inuvik	0.73	0.59	0.44	0.24	0.00	0.00	0.00	0.12	0.27	0.53	0.68	0.78
London	0.57	0.52	0.47	0.40	0.34	0.31	0.32	0.38	0.44	0.50	0.55	0.58
Moose Jaw	0.60	0.53	0.46	0.38	0.30	0.25	0.29	0.34	0.43	0.50	0.58	0.61
Whitehorse	0.65	0.56	0.45	0.32	0.18	0.00	0.1[illegible]	0.27	0.40	0.53	0.62	0.68
Cold Lake	0.61	0.54	0.46	0.36	0.27	0.20	0.23	0.32	0.42	0.51	0.59	0.63

2.6 Satellite Elevation Constraint. The probability of event *D*, $P(D)$, is the fraction of time the satellite is above an elevation of 15° above the horizon. Since geostationary satellites have a fixed location relative to an observer on the ground, this probability will be binary (either zero or one) and constant. Since these satellites are positioned over the Equator, only a latitude is necessary to specify position. Because of the extreme northern locations of the proposed stations, the elevation angles for all geostationary orbits will be small. In fact, $P(D)=0$ for all orbits at Alert and Inuvik. Table 4 depicts $P(D)$ at each site for the polar-orbiting navigational satellite.

TABLE 3. Mean fraction of time that a satellite in the navigational orbit is visible at each station.

STATION	PROBABILITY
Sandspit	0.28
Penticton	0.27
Churchill	0.30
Torbay	0.27
Alert	0.33
Frobisher	0.31
Inuvik	0.32
London	0.26
Moose Jaw	0.26
White Horse	0.31
Cold Lake	0.29

2.7 Temperature and Wind Speed Constraints. The probability of conditions B (surface wind speed less than 25 knots) and C (temperature below -50° C) can be determined from archived weather observations. USAFETAC's automated database has a period of record (POR) of 1973-1989. All but one one of the twelve stations in this study reported observations hourly; Alert reported only every 3 hours. During the 17-year POR, no observations lower than -50° C occurred. Research of the literature revealed that in the POR 1951-1980, temperatures below -50° C occurred at only two of the stations: Inuvik and Alert (Environment Canada, 1982). Even at these two stations, such temperatures are extremely rare; therefore, $P(C)$ is effectively unity for all twelve sites.

The value of $P(B)$ can also be obtained from weather observations. Table 4 lists the monthly probability of condition B given condition A, $P(B/A)$, for each location. Since $P(C)$=1, this table can also be considered the joint probability of conditions B and C, $P(BC/A)$.

TABLE 4. Fraction of time wind speeds are less than 25 knots given that the Sun is at least 6 degrees below the horizon. (The notation "----" indicates that the sun is *never* at least 6 degrees below the horizon.)

	JAN	FEB	MAR	APR	MAY	JUN	JUL	AUG	SEP	OCT	NOV	DEC
Sandspit	0.86	0.88	0.92	0.94	0.95	0.97	0.98	0.99	0.96	0.91	0.88	0.88
Churchill	0.89	0.92	0.93	0.94	0.96	0.97	0.97	0.95	0.91	0.87	0.88	0.90
Penticton	0.97	0.97	0.98	0.99	0.99	0.99	0.99	0.99	0.99	0.98	0.96	0.96
Chatham	0.96	0.96	0.96	0.97	0.99	0.99	0.99	0.99	0.99	0.99	0.97	0.96
Torbay	0.71	0.71	0.72	0.84	0.90	0.90	0.91	0.95	0.90	0.84	0.77	0.71
Alert	0.97	0.97	0.98	----	----	----	----	----	0.95	0.97	0.97	0.96
Frobisher	0.93	0.90	0.96	0.97	0.97	----	----	0.98	0.97	0.95	0.93	0.95
Inuvik	0.99	0.99	0.99	0.99	----	----	----	0.99	0.99	0.99	0.99	0.99
London	0.95	0.97	0.97	0.97	0.99	0.99	0.99	0.99	0.99	0.99	0.97	0.96
Moose Jaw	0.96	0.97	0.97	0.98	0.98	0.98	0.99	0.99	0.98	0.98	0.98	0.97
Whitehorse	0.97	0.97	0.99	0.99	0.99	----	0.99	0.99	0.99	0.97	0.97	0.96
Cold Lake	0.99	0.99	0.99	0.99	0.99	0.99	0.99	0.99	0.99	0.99	0.99	0.99

2.8 Conditional 5-minute CFLOS Probabilities. Next we will consider the probability of a 5-minute CFLOS (condition *E*) given conditions *A*, *B*, *C*, and *D*, *P(E/ABCD)*. Additional considerations are required to evaluate this conditional probability. Event *A* can be accounted for by merely excluding those cases between BMCT and EECT. Event *C* does not pose a problem since *P(C)*=1. Therefore, *P(E/ABCD)* = *P(E/ABD)*. Condition *D* is not a problem, either, since the simulation model keeps track of the satellite elevation, one of the two variables in the SRI CFLOS model. Event *B*, however, does present problems in that USAFETAC does not currently have a simulation model for both cloud cover and wind speed. Although such a model could be developed, it would have taken too long to be useful in supporting this project. If wind speeds and CFLOS probabilities are correlated, the simulation model would have to account for this, thereby increasing its complexity. However, if they are uncorrelated, then *P(E/ABD)* = *P(E/AD)*. If this is the case, the current CFLOS model could be used without modification to compute the required probabilities.

2.8.1 Correlation of Wind Speed and Cloud Cover. Since CFLOS calculation is based on mean sky cover, we studied the correlation of wind speed and mean sky cover. The study was restricted to stations at which the monthly probability of wind speeds greater than 25 knots was more than 5% of the time, given that the sun is at least 6 degrees below the horizon (see Table 4). Four stations met this criterion (Sandspit, 8 months; Churchill, 8 months; Frobisher, 4 months; Torbay, 12 months). Table 5 is a breakdown of observed clear, scattered, broken, and overcast skies for all hours, as well as for only those hours when wind speed exceeded 25 knots. A chi-square test was then conducted to test the null hypothesis that the distributions are the same; a plot of the various chi-square statistic values is given in Figure 3. Also shown is the level of significance at a confidence level of 95%. For most of the cases, the test rejected the null hypothesis, implying that wind speed and cloud cover are correlated; that is, *P(E/ABD)* ≠ *P(E/AD)*.

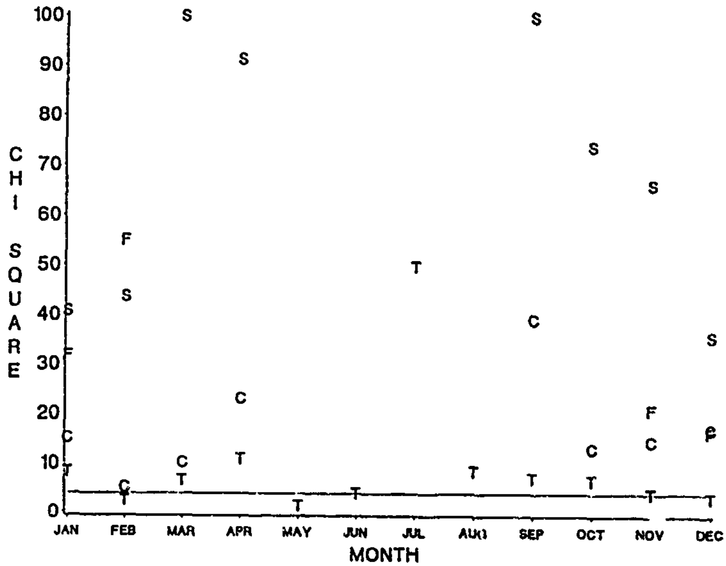

Figure 3. Values of chi-square statistics comparing the unconditional cloud-cover distribution with the conditional distribution when winds exceed 25 knots. The solid line is the 95% level of confidence. Plotted letters refer to locations; S--Sandspit, F--Frobisher, C-Churchill, T-Torbay.

Table 5. Comparison of airways cloud cover distributions, winds greater than 25 knots and all cases, for four of the proposed station locations.

	Wind > 25 Knots				All Cases			
Sandspit	CLR	SCT	BKN	OVC	CLR	SCT	BKN	OVC
January	0.01	0.05	0.13	0.81	0.06	0.20	0.24	0.50
February	0.04	0.05	0.15	0.76	0.09	0.22	0.25	0.44
March	0.02	0.04	0.09	0.85	0.09	0.29	0.25	0.37
April	0.00	0.06	0.11	0.83	0.10	0.28	0.25	0.37
September	0.02	0.01	0.11	0.86	0.14	0.28	0.26	0.32
October	0.00	0.05	0.13	0.82	0.07	0.28	0.25	0.40
November	0.01	0.04	0.15	0.80	0.05	0.28	0.27	0.40
December	0.01	0.09	0.15	0.75	0.05	0.25	0.24	0.46

	Wind > 25 Knots				All Cases			
Churchill	CLR	SCT	BKN	OVC	CLR	SCT	BKN	OVC
January	0.24	0.12	0.17	0.46	0.32	0.22	0.16	0.30
February	0.29	0.17	0.17	0.37	0.35	0.23	0.13	0.29
March	0.37	0.14	0.09	0.40	0.33	0.21	0.14	0.27
April	0.06	0.16	0.16	0.62	0.21	0.21	0.17	0.41
September	0.02	0.05	0.12	0.82	0.07	0.17	0.25	0.51
October	0.02	0.05	0.12	0.80	0.06	0.14	0.16	0.64
November	0.06	0.09	0.15	0.70	0.13	0.17	0.16	0.53
December	0.21	0.13	0.14	0.52	0.29	0.22	0.16	0.33

	Wind > 25 Knots				All Cases			
Frobisher	CLR	SCT	BKN	OVC	CLR	SCT	BKN	OVC
January	0.15	0.10	0.17	0.58	0.27	0.23	0.18	0.32
February	0.14	0.11	0.10	0.64	0.29	0.24	0.17	0.30
November	0.12	0.10	0.13	0.65	0.15	0.19	0.23	0.43
December	0.23	0.14	0.13	0.50	0.23	0.26	0.18	0.33

	Wind > 25 Knots				All Cases			
Torbay	CLR	SCT	BKN	OVC	CLR	SCT	BKN	OVC
January	0.02	0.18	0.25	0.35	0.05	0.19	0.24	0.53
February	0.02	0.16	0.27	0.55	0.05	0.18	0.23	0.54
March	0.04	0.17	0.18	0.61	0.08	0.17	0.25	0.50
April	0.02	0.05	0.20	0.73	0.06	0.13	0.21	0.59
May	0.03	0.16	0.18	0.63	0.05	0.14	0.19	0.61
June	0.01	0.11	0.32	0.56	0.04	0.16	0.28	0.53
July	0.01	0.08	0.11	0.80	0.05	0.21	0.29	0.45
August	0.02	0.17	0.20	0.61	0.06	0.22	0.23	0.48
September	0.03	0.17	0.31	0.49	0.08	0.23	0.27	0.42
October	0.02	0.15	0.26	0.57	0.06	0.21	0.27	0.46
November	0.02	0.15	0.24	0.60	0.04	0.19	0.27	0.50
December	0.01	0.17	0.30	0.53	0.04	0.16	0.27	0.53

2.8.2 Estimating Conditional Probabilities. A method had to be devised to compute the conditional probability, and we took the following approach: In computing statistics for the Burger distribution (mean sky cover and scale distance), all observations with wind speeds above 25 knots were excluded. The probabilities subsequently computed were then assumed to represent the conditional probability $P(E/ABCD)$.

3. MODEL RESULTS

3.1 Five-Minute CFLOS Probabilities. Tables 6 through 11 give monthly 5-minute CFLOS conditional probabilities, *P(E/ABCD)*, for six satellite configurations. Table 6 is for the 19,000 km orbit with a 65° angle of inclination. Tables 7 through 11 are for geostationary orbits with the satellite at the following positions (degrees west longitude): 50°, 70°, 100°, 120°, 140°.

TABLE 6. Conditional Probability of a 5-minute CFLOS for an orbiting satellite in the navigational orbit.

	JAN	FEB	MAR	APR	MAY	JUN	JUL	AUG	SEP	OCT	NOV	DEC
Sandspit	0.28	0.31	0.38	0.37	0.32	0.31	0.28	0.38	0.37	0.33	0.34	0.30
Churchill	0.47	0.47	0.50	0.35	0.27	0.29	0.35	0.40	0.24	0.20	0.29	0.42
Penticton	0.14	0.21	0.35	0.39	0.38	0.45	0.48	0.52	0.46	0.42	0.19	0.15
Chatham	0.39	0.38	0.36	0.34	0.33	0.41	0.41	0.45	0.43	0.40	0.34	0.36
Torbay	0.21	0.19	0.27	0.26	0.22	0.26	0.29	0.29	0.32	0.25	0.23	0.20
Alert	0.51	0.48	0.50	----	----	----	----	----	0.21	0.37	0.45	0.54
Frobisher	0.44	0.46	0.43	0.39	0.16	----	----	0.19	0.21	0.19	0.30	0.44
Inuvik	0.43	0.43	0.51	0.42	----	----	----	0.31	0.23	0.22	0.37	0.42
London	0.20	0.27	0.32	0.36	0.39	0.47	0.50	0.47	0.46	0.36	0.23	0.19
Moose Jaw	0.42	0.40	0.41	0.49	0.51	0.52	0.54	0.58	0.46	0.48	0.41	0.38
Whitehorse	0.35	0.38	0.36	0.43	0.36	----	0.28	0.33	0.34	0.24	0.23	0.31
Cold Lake	0.35	0.35	0.34	0.34	0.31	0.31	0.35	0.38	0.32	0.36	0.28	0.31

TABLE 7. Conditional Probability of a 5-minute CFLOS for a geostationary satellite at a longitude of 50° W.

	JAN	FEB	MAR	APR	MAY	JUN	JUL	AUG	SEP	OCT	NOV	DEC
Sandspit	----	----	----	----	----	----	----	----	----	----	----	----
Churchill	----	----	----	----	----	----	----	----	----	----	----	----
Penticton	----	----	----	----	----	----	----	----	----	----	----	----
Chatham	0.44	0.42	0.41	0.42	0.40	0.47	0.52	0.51	0.49	0.46	0.41	0.43
Torbay	0.27	0.23	0.31	0.33	0.27	0.31	0.39	0.32	0.35	0.31	0.29	0.25
Alert	----	----	----	----	----	----	----	----	----	----	----	----
Frobisher	0.48	0.47	0.45	0.45	0.19	----	----	0.20	0.24	0.21	0.34	0.49
Inuvik	----	----	----	----	----	----	----	----	----	----	----	----
London	0.25	0.30	0.36	0.45	0.45	0.54	0.60	0.52	0.52	0.42	0.28	0.24
Moose Jaw	----	----	----	----	----	----	----	----	----	----	----	----
Whitehorse	----	----	----	----	----	----	----	----	----	----	----	----
Cold Lake	----	----	----	----	----	----	----	----	----	----	----	----

TABLE 8. Conditional Probability of a 5-minute CFLOS for a geostationary satellite at a longitude of 70° W.

	JAN	FEB	MAR	APR	MAY	JUN	JUL	AUG	SEP	OCT	NOV	DEC
Sandspit	----	----	----	----	----	----	----	----	----	----	----	----
Churchill	0.51	0.50	0.54	0.43	0.31	0.34	0.45	0.42	0.28	0.23	0.33	0.48
Penticton	0.17	0.23	0.37	0.46	0.42	0.49	0.59	0.56	0.50	0.45	0.23	0.17
Chatham	0.43	0.42	0.41	0.43	0.39	0.47	0.52	0.51	0.49	0.45	0.42	0.42
Torbay	0.27	0.23	0.30	0.34	0.27	0.31	0.39	0.32	0.37	0.30	0.30	0.25
Alert	----	----	----	----	----	----	----	----	----	----	----	----
Frobisher	0.47	0.48	0.45	0.45	0.20	----	----	0.20	0.24	0.21	0.34	0.49
Inuvik	----	----	----	----	----	----	----	----	----	----	----	----
London	0.25	0.31	0.37	0.46	0.45	0.55	0.62	0.53	0.52	0.42	0.28	0.25
Moose Jaw	0.44	0.39	0.44	0.54	0.48	0.55	0.60	0.60	0.50	0.50	0.43	0.41
Whitehorse	----	----	----	----	----	----	----	----	----	----	----	----
Cold Lake	0.38	0.38	0.37	0.42	0.36	0.36	0.44	0.42	0.37	0.42	0.32	0.36

Table 9. Conditional Probability of a 5-minute CFLOS for a geostationary satellite at a longitude of 100° W.

	JAN	FEB	MAR	APR	MAY	JUN	JUL	AUG	SEP	OCT	NOV	DEC
Sandspit	0.31	0.33	0.41	0.44	0.33	0.34	0.33	0.39	0.40	0.36	0.36	0.35
Churchill	0.51	0.49	0.55	0.44	0.32	0.33	0.44	0.44	0.28	0.23	0.34	0.47
Penticton	0.19	0.28	0.40	0.49	0.45	0.53	0.61	0.58	0.52	0.48	0.25	0.19
Chatham	0.44	0.41	0.40	0.41	0.39	0.47	0.52	0.50	0.49	0.45	0.40	0.42
Torbay	0.26	0.21	0.29	0.31	0.25	0.29	0.36	0.30	0.33	0.27	0.26	0.23
Alert	----	----	----	----	----	----	----	----	----	----	----	----
Frobisher	----	----	----	----	----	----	----	----	----	----	----	----
Inuvik	----	----	----	----	----	----	----	----	----	----	----	----
London	0.24	0.30	0.37	0.46	0.45	0.54	0.62	0.53	0.51	0.42	0.28	0.22
Moose Jaw	0.47	0.41	0.45	0.55	0.51	0.57	0.62	0.59	0.51	0.51	0.44	0.44
Whitehorse	0.37	0.40	0.38	0.49	0.41	----	0.34	0.33	0.37	0.26	0.26	0.34
Cold Lake	0.41	0.40	0.40	0.45	0.39	0.39	0.47	0.45	0.40	0.43	0.35	0.38

Table 10. Conditional Probability of a 5-minute CFLOS for a geostationary satellite at a longitude of 120°W.

	JAN	FEB	MAR	APR	MAY	JUN	JUL	AUG	SEP	OCT	NOV	DEC
Sandspit	0.33	0.37	0.43	0.45	0.35	0.36	0.35	0.40	0.41	0.37	0.37	0.35
Churchill	0.51	0.50	0.54	0.43	0.31	0.33	0.44	0.42	0.28	0.22	0.34	0.47
Penticton	0.20	0.26	0.41	0.48	0.47	0.53	0.61	0.60	0.54	0.50	0.26	0.21
Chatham	0.40	0.40	0.37	0.40	0.37	0.43	0.49	0.47	0.45	0.43	0.37	0.39
Torbay	----	----	----	----	----	----	----	----	----	----	----	----
Alert	----	----	----	----	----	----	----	----	----	----	----	----
Frobisher	----	----	----	----	----	----	----	----	----	----	----	----
Inuvik	----	----	----	----	----	----	----	----	----	----	----	----
London	0.25	0.33	0.37	0.45	0.45	0.53	0.60	0.51	0.50	0.41	0.27	0.24
Moose Jaw	0.45	0.40	0.45	0.55	0.51	0.56	0.62	0.60	0.52	0.50	0.45	0.44
Whitehorse	0.39	0.42	0.40	0.52	0.41	----	0.36	0.35	0.39	0.29	0.27	0.36
Cold Lake	0.41	0.40	0.40	0.45	0.39	0.39	0.47	0.45	0.40	0.43	0.35	0.38

Table 11. Conditional Probability of a 5-minute CFLOS for a geostationary satellite at a longitude of 140° W.

	JAN	FEB	MAR	APR	MAY	JUN	JUL	AUG	SEP	OCT	NOV	DEC
Sandspit	0.33	0.33	0.43	0.45	0.35	0.35	0.35	0.41	0.41	0.37	0.37	0.35
Churchill	0.49	0.47	0.52	0.40	0.30	0.29	0.41	0.40	0.25	0.21	0.32	0.45
Penticton	0.18	0.24	0.41	0.50	0.45	0.52	0.61	0.59	0.53	0.48	0.25	0.19
Chatham	----	----	----	----	----	----	----	----	----	----	----	----
Torbay	----	----	----	----	----	----	----	----	----	----	----	----
Alert	----	----	----	----	----	----	----	----	----	----	----	----
Frobisher	----	----	----	----	----	----	----	----	----	----	----	----
Inuvik	----	----	----	----	----	----	----	----	----	----	----	----
London	----	----	----	----	----	----	----	----	----	----	----	----
Moose Jaw	0.44	0.39	0.44	0.55	0.49	0.55	0.60	0.60	0.50	0.49	0.43	0.42
Whitehorse	0.39	0.41	0.41	0.52	0.42	----	0.38	0.37	0.39	0.28	0.27	0.37
Cold Lake	0.39	0.38	0.38	0.44	0.37	0.37	0.46	0.44	0.38	0.42	0.33	0.37

3.1.1 How to Use the Tables. Data provided in the various tables can be used to calculate the joint probability of all five of the conditions *A-E*. From the definition of conditional probability, several expressions can be obtained:

$$P(ABCDE) = P(E/ABCD) \cdot P(ABCD) \tag{5}$$

$$P(ABCD) = P(D/ABC) \cdot P(ABC) \tag{6}$$

$$P(ABC) = P(C/AB) \cdot P(AB) \tag{7}$$

$$P(AB) = P(B/A) \cdot P(A) \tag{8}$$

Substituting (6) into (5) yields:

$$P(ABCDE) = P(E/ABCD) \cdot P(D/ABC) \cdot P(ABC) \tag{9}$$

Combining this expression with (7) and (8) results in:

$$P(ABCDE) = P(E/ABCD) \cdot P(D/ABC) \cdot P(C/AB) \cdot P(B/A) \cdot P(A) \tag{10}$$

Event D is independent of events A, B, and C and as a result we can state as $P(D/ABC) = P(D)$. Also, since $P(C)=1$, the conditional probability of C occurring will always be unity, $P(C/AB)=1$. Therefore, the final result is:

$$P(ABCDE) = P(E/ABCD) \cdot P(D) \cdot P(B/A) \cdot P(A) \tag{11}$$

Another useful expression, derived in a similar manner, is the probability of being able to detect a satellite in the navigational orbit given that it is within view, $P(ABCE/D)$:

$$P(ABCE/D) = P(E/ABCD) \cdot P(B/A) \cdot P(A) \tag{12}$$

3.1.2 Sample Calculation. To compute the probability that a satellite in the 19,000-km navigational orbit can be detected by the GEODSS system at Torbay during January given that the satellite elevation angle is at least 15°, first obtain values for each term in equation 12 from the tables:

- Get $P(A)$ from Table 3 (0.58)
- Get $P(B/A)$ from Table 5 (0.71).
- Get $P(E/ABCD)$ from Table 7 (0.21)

Multiplying these numbers together gives 0.09; therefore, there is only a 9% chance that weather conditions will permit detection of the satellite when it is in view. In contrast, the probability at Alert during January is 49%. Table 12 lists probabilities by month for all 11 stations.

TABLE 12. Conditional probabilities of joint occurrences of conditions *A, B, C, and E,* given condition D. Condition A--Sun at least 6 degrees below the horizon; B--surface wind speeds less than 25 knots; C--temperature higher than -50° C; D--satellite's elevation angle at least 15° above the horizon; and E--5-minute CFLOS between an object in a 19,000 km orbit (right ascension angle of 65°) and the ground.

	JAN	FEB	MAR	APR	MAY	JUN	JUL	AUG	SEP	OCT	NOV	DEC
Sandspit	0.15	0.15	0.16	0.11	0.09	0.07	0.07	0.12	0.15	0.15	0.18	0.17
Churchill	0.27	0.24	0.21	0.11	0.06	0.06	0.08	0.11	0.09	0.09	0.16	0.25
Penticton	0.08	0.11	0.16	0.15	0.12	0.12	0.14	0.18	0.20	0.21	0.10	0.09
Chatham	0.22	0.20	0.16	0.13	0.13	0.11	0.12	0.16	0.18	0.20	0.19	0.21
Torbay	0.09	0.07	0.09	0.09	0.06	0.07	0.08	0.10	0.12	0.11	0.10	0.09
Alert	0.49	0.40	0.16	0.00	0.00	0.00	0.00	0.00	0.03	0.22	0.44	0.52
Frobisher	0.28	0.24	0.19	0.11	0.02	0.00	0.00	0.04	0.08	0.09	0.18	0.30
Inuvik	0.29	0.25	0.22	0.10	0.00	0.00	0.00	0.04	0.06	0.12	0.25	0.30
London	0.11	0.14	0.15	0.14	0.13	0.15	0.16	0.18	0.20	0.18	0.12	0.14
Moose Jaw	0.24	0.21	0.14	0.13	0.15	0.13	0.16	0.16	0.19	0.24	0.23	0.22
Whitehorse	0.22	0.21	0.16	0.14	0.06	0.00	0.03	0.09	0.13	0.12	0.14	0.20
Cold Lake	0.21	0.19	0.16	0.12	0.08	0.06	0.08	0.12	0.13	0.18	0.16	0.19

3.2 Differences in the Various Tables. Since all the proposed stations are at far northern latitudes, the elevation angle of the satellites for the geostationary orbits will always be low. As a result, CFLOS probabilities differ only slightly among the various geostationary positions.

4. DISCUSSION

4.1 Evaluation of Model Results. Evaluation of the probabilities provided by this simulation is difficult because databases of *observed* occurrences of CFLOS are limited. In place of this type of comparison, tests can be conducted on the data to ensure the results are consistent with the basic assumptions of the model.

4.2 Relationship between Mean Monthly 5-Minute CFLOS Probabilities and Mean Sky Cover. Figure 4 is a scatterplot of monthly mean sky cover (computed only from those observations when the Sun is at least 6 degrees below the horizon) versus the monthly mean 5-minute CFLOS probability, *P(E/ABCD)*, for the 19,000 km navigational orbit. The plot indicates a very large linear correlation between these two variables (correlation coefficient of -0.98). Also shown in Figure 4 are the CFLOS probabilities from the SRI CFLOS model. These values are point probabilities based on a 40° elevation angle, the average elevation of the orbiting satellite. The difference between the curve and the plotted data primarily reflects the effect of the 5-minute window on the degradation of CFLOS probabilities. A typical value of this degradation is 8%; it is somewhat larger for the smaller values of mean sky cover and somewhat smaller for the larger values.

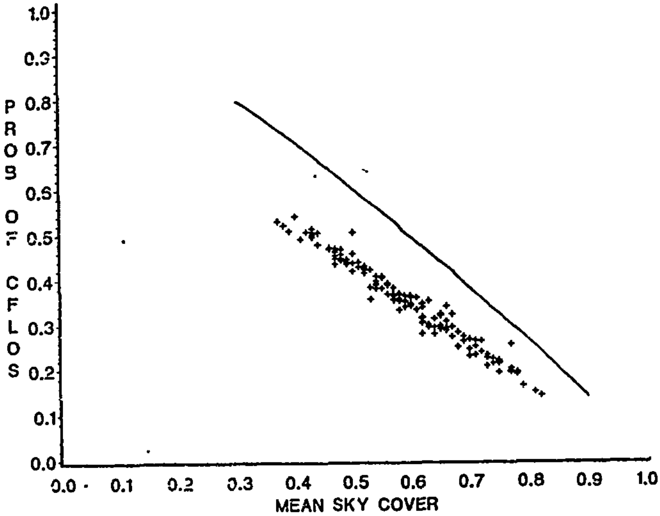

Figure 4. Relationship of mean monthly sky cover with monthly 5-minute CFLOS probabilities.

4.3 Relationship between CFLOS Degradation and Sky-Dome Scale Distance. We define the term "CFLOS degradation" as the difference between the point and 5-minute CFLOS probabilities. Figure 5 is a plot of CFLOS degradation versus sky dome scale distance. The correlation coefficient of these two variables is -0.74. This type of correlation is consistent with our fundamental assumptions. A short scale distance suggests that hour-to-hour values of cloud cover show considerable fluctuation (cumuliform clouds), while a large scale distance suggests more consistent hour-to-hour values (straiform clouds). With a large scale distance, cloud cover tends to be either totally clear or cloudy. Therefore, if a 5-minute interval begins with a cloud-free line-of-sight, it is likely to remain clear for the duration; degradation is small. With a small scale distance, cloud cover tends more toward intermediate values (partly cloudy). Clouds tend to be scattered across the sky, increasing the probability of encountering a cloud at some time during the 5-minute interval and increasing degradation. The plots in both Figures 4 and 5 suggest that the CFLOS statistics are consistent with the fundamental assumption made in using the Burger distribution and the SRI CFLOS model.

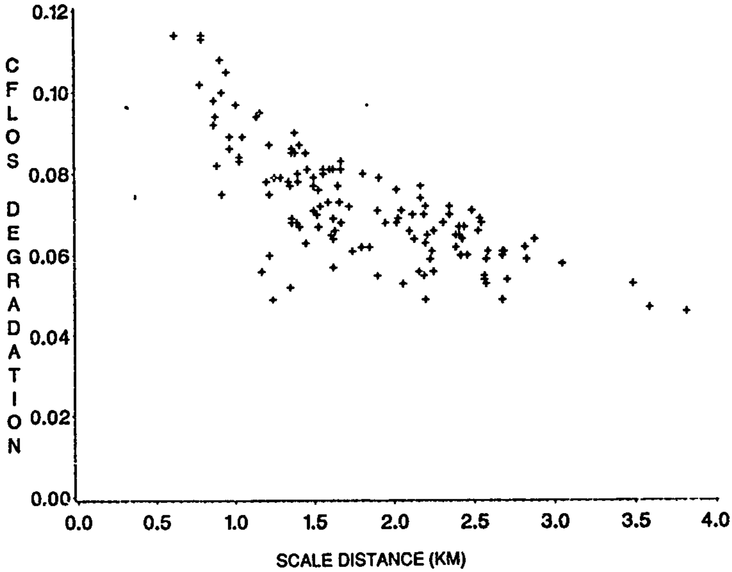

Figure 5. Relationship of the difference in point CFLOS probabilities and 5-minute CFLOS probabilities (CFLOS degradation) with the sky-dome scale distance.

5. CONCLUSIONS

5.1 Summary of Results. Weather is not the only consideration in selecting the best location for a GEODSS sensor. But based only on the results of this environmental study, Moose Jaw stands out as the best choice; winds are seldom over 25 knots, CFLOS conditional probabilities are consistently among the highest for all 12 months, and its southern location allows the system to be operational during the summer months.

Alert would be a very good choice for detecting objects in the navigational orbit between November and March. The joint probability, *P(ABCDE)*, in December is 17% at Alert versus 6% at Moose Jaw. However, the probability is zero from April through August. For geostationary orbits, it is zero for all 12 months.

Torbay appears to be the worst choice. During the winter, winds in excess of 25 knots occur about 30% of the time. Throughout the years Torbay's conditional CFLOS probabilities are consistently near the bottom of the group.

5.2 Final Point. This study provided a good example of how simulation modeling can be used to estimate event probabilities when direct observations are not available. One of the advantages of this type of modeling is the relative ease in linking several different models together, as was done here with the CLDGEN and satellite orbit models. The data clearly shows the differences and similarities in the 12 proposed sites, and will help decision-makers pick the best possible site for the GEODSS system.

BIBLIOGRAPHY

Boehm, A.R., *Transnormalized Regression Probabilities*, AWS-TR-75-259, Air Weather Service, Scott AFB, IL, 1975.

Burger, C.F., *World Atlas of Total Sky-Cover*, AFGL-TR-85-0198, Air Force Geophysics Laboratory, Hanscom AFB, MA, 1985.

Environment Canada, *Canadian Climate Normals 1951-1980*, Vols 1-6, 1982.

Gringorten, I.I. and A.R. Boehm, *The 3D-BSW Model Applied to Climatology of Small Areas and Lines*, AFGL-TR-0251, Air Force Geophysics Laboratory, Hanscom AFB, MA, 1987.

Hering, W.S., *Evaluation of Stochastic Models for Estimating the Persistence Probability of Cloud-Free Lines-of-Sight*, AFGL-TR-89-0275, Air Force Geophysics Laboratory, Hanscom AFB, MA, 1989.

Malick, J.D., J.H. Allen, S. Zakanycz, *"Calibrated Analytical Modeling of Cloud-Free Intervals,"* SPIE Vol 195: Atmospheric Effects on Radiative Transfer, pp. 142-147, 1979.

Rupp, J.A., *CLDGEN Users Guide*, USAFETAC/TN-90/003, United States Air Force Environmental Technical Applications Center, Scott AFB, IL, 1990.

Whiton R.C. and E.M. Bereeck, *Basic Techniques in Environmental Simulation*, USAFETAC/TN-82/004, United States Air Force Environmental Technical Applications Center, Scott AFB, IL, 1982.

ACRINABs

ACRINAB	Acronym, initialism, or abbreviation
BMCT	Beginning of morning civil twilight
CFLOS	Cloud-free line-of-sight
CLDGEN	Cloud scene generator model
EECT	End of evening civil twilight
END	Equivalent normal deviate
GEODSS	Ground-based electrooptical deep-space surveillance
MSL	Mean sea level
NDHQ	Canadian National Defence Headquarters
SRI	Stanford Research Institute
SSC	Space Surveillance Center
USAFETAC	US Air Force Environmental Technical Applications Center
USSPACECOM	US Space Command
USSPACECOMR	USSPACECOM Regulation

DISTRIBUTION

AWS/DO/PM/SC/XT, Scott AFB, IL 62225-5008	1
SAF/SS/PO, Rm 4C1052, Pentagon, Washington, DC 20330-6560	1
OL A, AFCOS, Ft Ritchie, MD 21719-5010	1
OL-B, HQ AWS, Hanscom AFB, MA 01731-5000	1
CSTC/WE, PO Box 3430, Onizuka AFB, CA 94088-3430	1
OD-4/DX, Onizuka AFB, CA 94088-3430	1
Det 9, HQ AWS, PO Box 12297, Las Vegas, NV 89112-0297	1
1SSD/WE (Stop 77), Buckley ANG Base, Aurora, CO 80011-9599	1
OL-B, HQ AWS, Hanscom AFB, MA 01731-5000	1
OL-E, HQ AWS, Ft Leavenworth, KS 66027-5310	1
SSD/MWA, PO Box 92960, Los Angeles, CA 90009-2960	1
OL-H, HQ AWS, Ft Huachuca, AZ 85613-7000	1
OL-I, HQ AWS, Ft Monroe, VA 23651-5000	1
OL-K, HQ AWS, NEXRAD Opnl Support Facility, 1200 Westheimer Dr., Norman, OK 73069	1
OL-M, HQ AWS, McClellan AFB, CA 95652-5609	1
AFGWC/SYSE MBB39, 106 Peacekeeper Dr., STE2N3, Offutt AFB, NE 68113-4039	3
USAFETAC, Scott AFB, IL 62225-5438	6
1WW/DN, Hickam AFB, HI 96853-5000	1
11WS/DON, 6900 9th St, Suite 205, Elmendorf AFB, AK 99506-2250	1
20WS/DON, APO AP 96328-5000	1
30WS/DON, APO AP 96301-0420	1
2WW/DN, APO AE 09094-5000	1
7WS/DON, APO AE 09403-5000	1
28WS/DON, APO AE 09127-5000	1
31WS/DON, APO AE 09136-5000	1
HQ SAC/DOW, 901 SAC Blvd, Suite M13, Offutt AFB, NE 68113-5340	1
4WW/DN, Peterson AFB, CO 80914-5000	1
2WS/DON, Andrews AFB, MD 20334-5000	21
5WW/DN, Langley AFB, VA 23665-5000	1
1WS/DON, MacDill AFB, FL 33608-5000	1
3WS/DON, Shaw AFB, SC 29152-5000	1
5WS/DON, Ft McPherson, GA 30330-5000	1
25WS/DON, Bergstrom AFB, TX 78743-5000	1
7WW/DN, Scott AFB, IL 62225-5008	1
6WS/DON, Hurlburt Field, FL 32544-5000	1
15WS/DON, McGuire AFB, NJ 08641-5002	1
17WS/DON, Travis AFB, CA 94535-5986	1
3350 TCHTG/TTGU-W, Stop 62, Chanute AFB, IL 61868-5000	1
3395 TCHTG/TTKO-W, Keesler AFB, MS 39534-5000	1
AFIT/CIR, Wright-Patterson AFB, OH 45433-6583	1
COMNAVOCEANCOM, Code N312, Stennis Space Ctr, MS 39529-5000	1
NAVOCEANO (Rusty Russum), Stennis Space Ctr, MS 39522-5001	1
NAVOCEANO, Code 9220 (Tony Ortolano), Stennis Space Ctr, MS 39529-5001	1
Maury Oceanographic Library (NOC), Code XJL, Stennis Space Ctr, MS 39529-5001	1
FLENUMOCEANCEN, Monterey, CA 93943-5006	1
NOARL West, Monterey, CA 93943-5006	1
Naval Research Laboratory, Code 4323, Washington, DC 20375	1
Naval Postgraduate School, Chmn, Dept of Meteorology, Code 63, Monterey, CA 93943-5000	1
Naval Eastern Oceanography Ctr (Clim Section), U117 McCAdy Bldg, Norfolk NAS, Norfolk, VA 23511-5000	1
Naval Western Oceanography Ctr, Box 1.3, Attn: Tech Library, Pearl Harbor, HI 96860-5000	1

Naval Oceanography Command Ctr, COMNAVMAR Box 12, FPO AP CA 96630-5000 1
Naval Oceanography Command Ctr, Box 31, USNAVSTA FPO AE NY 09540-3000 1
Pacific Missile Test Center, Geophysics Division, Code 3253, Pt Mugu, CA 93042-5000..1
Dept of Commerce/NOAA/MASC Library MC5 (Jean Bankhead), 325 Broadway, Boulder, CO 80303 1
OFCM, Suite 900, 6010 Executive Blvd, Rockville, MD 20852 1
NOAA Library-EOC4WSC4, Attn: ACQ, 6009 Executive Blvd, Rockville, MD 20852..1
NOAA/NESDIS (Attn: Nancy Everson, E/RA22), World Weather Bldg, Rm 703, Washington, DC 20233 1
NOAA/NESDIS (Attn: Capt Pereira, E/SP1), FB #4, Rm 0308, Washington, DC 20233-0001 1
Armed Forces Medical Intelligence Agency, Info Svcs Div., Bldg 1607, Ft Detrick, Frederick, MD 21701-5004 1
PL OL-AA/SULLA, Hanscom AFB, MA 01731-5000..1
PL GD/LYA, Hanscom AFB, MA 01731-5000 1
Atmospheric Sciences Laboratory (SLCAS-AT-AB), Aberdeen Proving Grounds, MD 21005-5001 1
Atmospheric Sciences Laboratory (SLCAS-AS-I 310-2c), White Sands Missile Range, NM 88002-5501 1
TECOM Atmos Sci Div, Attn: AMSTE-TC-AA (MacBlain), White Sands Missile Range, NM 88002-5504 1
Army Missile Command, ATTN: AMSMI-RD-TE-F, Redstone Arsenal, AL 35898-5250 1
Army Test & Eval Cmd, ATTN: AMSTE-TC-AM (RE) TCOM Met Team, Redstone Arsenal, AL 35898-8052.......1
Commander and Director, U.S. Army CEETL, Attn: GL-AE, Fort Belvoir, VA 22060-5546..1
6510 TESTW/TSTL, Edwards AFB, CA 93523-5000 1
RL/DOVL, Bldg 106, Griffiss AFB, NY 13441-5700..1
AFESC/RDXT, Bldg 1120, Stop 21, Tyndall AFB, FL 32403-5000..1
Technical Library, Dugway Proving Ground, Dugway, UT 84022-5000 1
NWS W/OSD, Bldg SSM C-2 East-West Hwy, Silver Spring, MD 20910..1
NCDC Library (D542X2), Federal Building, Asheville, NC 28801-2723..1
NIST Pubs Production, Rm A-405, Admin Bldg, Gaithersburg, MD 20899 1
Maj Pete Forgues, Canadian School of Aerospace Studies, CFB Winnipeg, Westwin, Manitoba,
Canada R3J-OTO 3
DTIC-FDAC, Cameron Station, Alexandria, VA 22304-6145..2
AUL/LSE, Maxwell AFB, AL 36112-5564..1
AWSTL, Scott AFB, IL 62225-5438..35